Boundary-Layer Meteorol (2008) 127:449–467
DOI 10.1007/s10546-008-9267-0

ORIGINAL PAPER

Eddy-Covariance Flux Measurements in the Complex Terrain of an Alpine Valley in Switzerland

Rebecca Hiller · Matthias J. Zeeman · Werner Eugster

Received: 12 June 2007 / Accepted: 4 February 2008 / Published online: 28 February 2008

Abstract We measured the surface energy budget of an Alpine grassland in highly complex terrain to explore possibilities and limitations for application of the eddy-covariance technique, also for CO_2 flux measurements, at such non-ideal locations. This paper focuses on the influence of complex terrain on the turbulent energy measurements of a characteristic high Alpine grassland on Crap Alv (Alp Weissenstein) in the Swiss Alps during the growing season 2006. Measurements were carried out on a topographic terrace with a slope of 25° inclination. Flux data quality is assessed via the closure of the energy budget and the quality flag method used within the CarboEurope project. During 93% of the time the wind direction was along the main valley axis (43% upvalley and 50% downvalley directions). During the transition times of the typical twice daily wind direction changes in a mountain valley the fraction of high and good quality flux data reached a minimum of ≈50%, whereas during the early afternoon ≈70% of all records yielded good to highest quality (CarboEurope flags 0 and 1). The overall energy budget closure was 74 ± 2%. An angular correction for the shortwave energy input to the slope improved the energy budget closure slightly to 82 ± 2% for afternoon conditions. In the daily total, the measured turbulent energy fluxes are only underestimated by around 8% of net radiation. In summary, our results suggest that it is possible to yield realistic energy flux measurements under such conditions. We thus argue that the Crap Alv site and similar topographically complex locations with short-statured vegetation should be well suited also for CO_2 flux measurements.

R. Hiller
Institute of Geography, University of Bern, Bern, Switzerland

Present Address:
R. Hiller
University of Minnesota, Saint Paul, MN 55108, USA
e-mail: hiller@umn.edu

M. J. Zeeman · W. Eugster (✉)
Institute of Plant Sciences, ETH Zurich, LFW C55.2, Universitaetsstrasse 2, 8092 Zurich, Switzerland
e-mail: werner.eugster@ipw.agrl.ethz.ch

Keywords Alpine grasslands · CarboEurope project · Complex terrain · Energy budget closure · Footprint model · Quality control · Valley wind system

1 Introduction

Over the last decade, the eddy-covariance (EC) method has become established as the method of choice to estimate the long-term net ecosystem exchange (NEE) of CO_2. Before, measurements were typically restricted to short-term campaigns due to a lack of appropriate instrumentation and data logging capabilities. To assess NEE, EC measurements have the advantage of being scale appropriate and surveying a whole ecosystem, whereas cuvette and chamber systems only capture a small part of it (Baldocchi 2003).

Nevertheless, the EC method also has limitations. The measurements are expected to be most accurate over flat terrain where there is an extended homogenous surface upwind from the tower, and when environmental conditions (wind, temperature, humidity and CO_2) are steady (Baldocchi 2003). Additionally, the one-dimensional approach of the EC method assumes that vertical turbulent exchange is the dominant flux, whereas advective influences should be negligible.

The strict requirements of eddy covariance are demanding even for ideal sites. Data from current sites in the global Fluxnet network have raised questions on the applicability of the EC method (Wilson et al. 2002). Although it has been demonstrated that measured fluxes are reproducible and are consistent when compared with the results of other methods carried out at the same location (Barr et al. 1994), this does not automatically imply that such measurements are highly accurate. The application of the EC method under less-than-ideal conditions, for example in complex terrain, and especially for long-term measurements, has yet to be fully explored. Hammerle et al. (2007) were among the first who successfully deployed the EC method under such challenging conditions.

General problems of the EC method are typically associated with thermal stratification at night, which leads to an underestimation of the ecosystem respiration as the required turbulent mixing can at times be reduced or intermittent. Conversely, the break-up of the nocturnal stable boundary layer vents the CO_2 stored in the canopy, causing an overestimation of the flux density during such periods (Baldocchi 2003). All these factors are not specific to complex terrain and should not per se preclude the application of the EC method for direct flux measurements. To answer ecological questions, namely quantification of NEE in unlevel terrain, it is actually important to explore possibilities to extend the applicability of the EC method to such non-ideal conditions.

Data from subalpine and alpine environments are rare (Rogiers 2005), particularly due to the fact that such mountainous areas do not conform to optimum conditions for measuring fluxes with the EC method. Our goal was to explore possibilities to measure the surface energy budget and net CO_2 exchange of an alpine grassland at the Alpine tree line in the Swiss Alps during the growing season 2006 using the EC method. The focus of this paper lies in the energy budget measurements and the assessment of the data quality with respect to the most relevant aspects in order to validate our EC flux measurements under such non-ideal conditions. By using various specific filters to screen out suspicious records and assess overall flux data quality according to the CarboEurope flagging standard we show that our energy flux measurements (sensible and latent heat) are of sufficiently high quality to be comparable with sites that appear to be located in more ideal terrain.

Fig. 1 Digital elevation model (DHM25) with superimposed aerial photograph (swisstopo). The yellow point indicates the study site. View is from the west looking east towards Albula pass (right from centre). Reproduced by permission of swisstopo (BA081029)

2 Methods

2.1 Site Description

The study area is located on Crap Alv (Alp Weissenstein) on the western side of the Albula pass in the Swiss Alps (47°34′59″N, 9°47′26″E) at about 2000 m a.s.l. (see Fig. 1). The alp is one of the three official agricultural ETH research stations and covers the alpine altitudinal belt of the traditional Swiss Alpine agricultural system (http://www.chamau.ethz.ch/weissenstein/index_EN).

The instruments were mounted on a flat terrace, which is terminated by slopes in the north and south and has neither sharp topographical discontinuities nor a sharp vegetation boundary within the measured fetch, with its largest extent along the valley axis. Moraines from the Val Bever glacier build the underlying material (Caflisch 1954) as well as limestone debris from the steep valley slopes that overlie the glacial formation (Bearth et al. 1987). The soil is composed of slightly humous to humous sandy loam (see M. Schärer (2003) Kurzbericht der Fallstudie Alp Weissenstein, Nährstoffanalysen in Alpweiden Sommer 2002, ETH Zürich, unpublished),[1] a typical composition for a fossil glacier foreland.

Shortly after the second world war this area had been ploughed for potato production (Caflisch 1954). Since then, the site has been a summer-grazed pasture. The current vegetation community of the research site itself was defined as Deschampsio cespitosae-Poetum alpinae whereas the slope above is classified as Trifolio thalii-Festucetum violoceae (Keller 2006). The vegetation achieved a maximum height of 0.40 m with an estimated maximum leaf area index of 4 $m^2\,m^{-2}$ before the grass cut, and around 0.10 m thereafter. The cut was performed in order to keep the vegetation within the fenced area as similar as possible to the cattle grazed area. This corresponds relatively well with the management of the pastures around as the livestock is normally moved on a regular base in order to provide them with fresh grass.

Climatologically, we find the typical inner and high alpine conditions of the Swiss Alps. They are specified as a comparably dry climate because of the barrier effect of the surrounding mountains. The weather conditions are dominated by winds from the Atlantic while the Mediterranean influence rarely occurs. Temperature and also the spatial precipitation

[1] Available from the authors.

distribution are mainly driven by the local environment specifying the microclimate. The snow cover on the south slopes typically lasts from the end of October until the beginning of May whereas the north slopes are snow-capped from the beginning of October to the beginning of June. The growing season lasts from mid May to the end of September, which is quite long for this altitude. Foehn periods during spring and autumn are the main reason for its extension to 4.5 months.

2.2 Instrumentation

We measured the water vapour and CO_2 fluxes using the eddy-covariance method from 23 June to 12 September 2006. The tower was equipped with a three-dimensional sonic anemometer for measuring wind speed, air temperature and wind direction (1012/R, Gill Ltd., Lymington, UK) and an open path IRGA (InfraRed Gas Analyser, LI-COR LI-7500, Lincoln, Nebraska, USA) for measuring carbon dioxide and water vapour concentrations. The instruments were mounted at 1.45 m above ground level (median roughness length $z_0 = 0.03$ m) giving a relatively small footprint. For data acquisition, we used an iPAQ PDA produced by Hewlett-Packard with an SD card extension as storage media running the *sonicread* software[2] on a Linux operating system similar to the system described by van der Molen et al. (2006). Three large batteries, each with a capacity of 56 Ah, powered the system and were partially recharged (≈50% of the actual demand) by two 21 W solar panels. The batteries were exchanged against fully charged ones every week.

Additionally, we ran a weather station from 23 June to 21 September, covering the same period during which eddy-covariance measurements were performed. The station was equipped with the following sensors: pluviometer (TE225-LC,Texas Electronics, Dallas, USA; 2 m above ground), pyranometer (SP LITE, Kipp & Zonen, Delft, The Netherlands; 2 m above ground), air temperature and relative humidity sensor (HygroClip, ROTRONIC AG, Bassersdorf, Switzerland; 2 m above ground), net radiometer (CNR1, Kipp & Zonen, Delft, The Netherlands; 1 m above ground) which was heated during morning hours with high relative humidity to prevent dewfall, photosynthetic photon flux density (PPFD) sensor (PAR LITE, Kipp & Zonen, Delft, The Netherlands; 1 m above ground), soil temperature sensor (TBMS1G, Campbell Scientific Inc., Loughborough, UK, 0.05 m below surface) and three soil heat flux plates (CN3, Middleton Solar, Melbourne, Australia, 0.02 m below surface). All variables were measured in 10-s intervals and afterwards averaged (precipitation totalised) to 10-min values, which were then stored on a data logger (CR10X, Campbell Scientific Inc., Loughborough, UK). Power supply was guaranteed by a 15 W solar panel connected to a 36 Ah capacity battery.

During a short time period (26 July to 3 August 2006), an additional soil respiration chamber of the type LI-8100 (LI-COR, Lincoln, Nebraska, USA) was installed between the EC instruments and the weather station.

2.3 Data Quality

The CarboEurope standard quality control is based on two tests to assess the fulfilment of the theoretical requirements for representative EC measurements. The first one is the steady-state test according to Foken and Wichura (1996). The calculated 30-min flux value of each component is compared to the respective average of the 5-min flux values for the same period. When the two values differ by less than 30%, the measurement is tagged as high quality data

[2] The source code for Unix/Linux systems can be obtained from the authors.

(flag 0). Measurements with differences of 30–100% are considered good (flag 1), whereas more than 100% deviation is flagged as not meeting the requirements (flag 2).

The second test is the integral turbulence characteristics test (Foken and Wichura 1996). Using the so-called flux-variance similarity (σ_w/u_*), the development of the turbulent conditions is assessed where σ_w is the standard deviation of the vertical wind speed, and u_* is the friction velocity. This ratio is once calculated from the measured data and once estimated by an empirical model using the Obukhov length, assuming that this ratio is independent of local topographic conditions and thus is an indicator of flux data quality. The class ranges for the percentage of differences between measured and modelled values are the same as for the steady-state test described above.

The outputs of both tests are combined and define the quality assessment/quality control flag. The *eth-flux* program[3] calculates the quality flag for both turbulent fluxes of water vapour and CO_2 separately and takes the higher flag value of the two tests for each component. In addition to this procedure we set the flag to poor quality (flag 2) whenever the momentum flux is not directed towards the surface (see Eugster et al. 2003).

2.4 Data Processing

The data from the eddy-covariance tower were evaluated and the fluxes calculated with the in-house *eth-flux* software. This program first rotates the coordinate system into the mean streamline for the averaging period and then eliminates $\overline{w}$ in a second rotation (McMillen 1988). After searching for the time lag with the highest correlation in between the two variables, the fluxes are calculated following the rules of Reynolds' averaging (Stull 1988). The time lag search was restricted to a time window from 0 to 0.5 s. This time lag is typically a function of wind direction and is influenced by instrument-inherent time delays and longitudinal sensor separation. For quality control, the program uses the official CarboEurope standard described in the previous section. This software also participated in the CarboEurope software intercomparison (Mauder et al. 2007).

In a next step, the data of the weather station and the eddy-covariance tower were merged and filtered using various crosschecks. First, we filtered out all the data where the difference between the air temperature measured by the sonic anemometer and the hygro clip of the weather station exceeded 5°C. This difference is assumed to be caused by an obstruction blocking the sonic path leading to invalid measurements. In this case, the data from the IRGA and the sonic were removed. Second, we rejected all measurements during periods with precipitation as during such weather conditions water drops covering the optical window of the IRGA lead to measurement errors. Third, we compared the measured water vapour concentration of the IRGA with that derived from the relative humidity of the air. When the difference exceeded the threshold of 100 mmol m^{-3}, we rejected the data as well. The last filter used the quality flags produced by the *eth-flux* software (see Sect. 2.3), only allowing data where the flag quality for CO_2 was lower than or equal to one (good and best quality).

After having rejected low quality measurements, the damping loss correction (Eugster and Senn 1995) and the Webb correction (Webb et al. 1980) were applied to the flux data. The damping loss correction describes the spectral loss in the high frequencies from the slightly modified formulation of the idealized model introduced by Kaimal et al. (1972) as described in Eugster and Senn (1995) using the model of an inductance in an alternating-current circuit. For our site, an inductance of $L = 0.15$ s could be found for both the CO_2 and the water vapour flux (see Fig. 2). This correction increased both fluxes about 12%. The Webb

[3] The source code for Unix/Linux systems can be obtained from the authors.

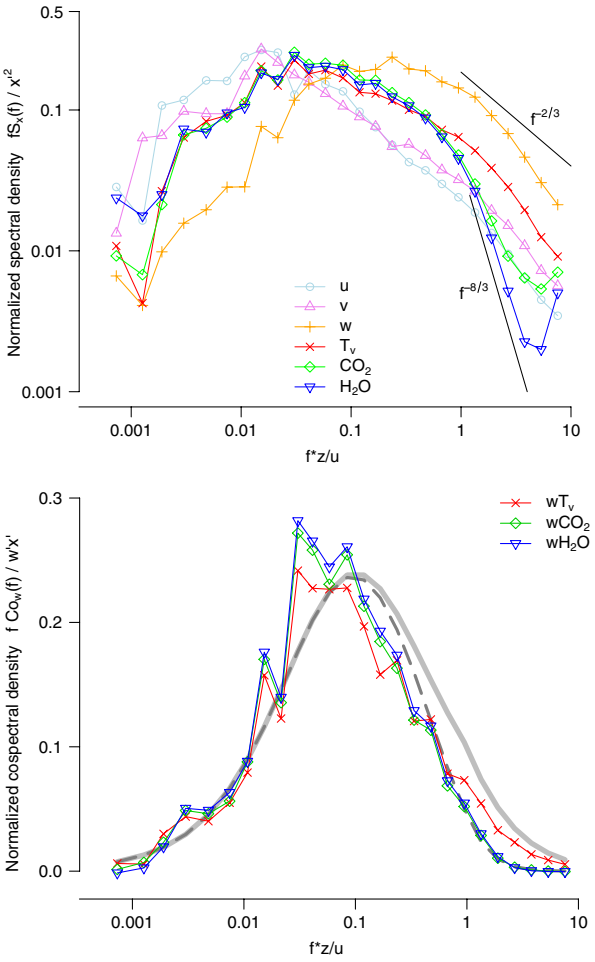

Fig. 2 Spectra (upper panel) and cospectra (lower panel) for September 12 2006 for the time 1200–1300 with $u = 1.62\,\mathrm{m\,s^{-1}}$ and $z/L = -0.35$. For the spectra, the slope –2/3 is shown for the undamped spectra and –8/3 for the damped, respectively. The solid grey line in the cospectra panel shows the idealised cospectra (based on Kaimal et al. 1972 as described in Eugster and Senn 1995) for the given environmental conditions wheras the dashed line indicates the damped idealised cospectra with $L = 0.15$ s

correction accounts for the fact that rising air parcels normally have a lower density than downwards moving ones, which leads to an apparent downward CO_2 flux. This correction reduces the magnitude of the CO_2 flux by 25% and increases the H_2O flux by 2.5%.

The data from the weather station were visually screened and unreliable values replaced with "no value". We corrected the precipitation data by around plus 10% according to a post-field calibration measurement. In addition, the data of the net radiometer were corrected after the sensor was intercalibrated next to an ASRB (Alpine Surface Radiation Budget) station of MeteoSchweiz at the World Radiation Center in Davos. Further, the storage terms of the soil heat, sensible heat and latent heat flux as well as of the CO_2 flux have been added to the corresponding fluxes.

2.5 Surface Radiation on an Inclined Surface

The intensity of direct radiation incident on inclined surfaces differs from that on horizontal surfaces as energy input depends on the angle of incidence. This dependency can be written as follows (Oke 1987):

$$S' = S\cos(\Theta) \tag{1}$$

where S is the radiant flux density perpendicular to the incident surface beam and Θ the angle between the direct beam and the normal to the slope surface. Θ not only depends on the inclination of the slope as the solar declination also modifies this parameter as well as the slope azimuth angle. Θ can be defined as the difference between β and Z, where β is the angle between the solar beam and the normal to the slope, whereas Z is the solar zenith angle (Whiteman et al. 1989).

Matzinger et al. (2003) presented an empiric relationship between the horizontally measured net radiation Q_* and the slope parallel measured Q'_*. As the quotient between the slope parallel and horizontally measured global radiation is proportional to that of the net radiation, Q'_* can be written as:

$$Q'_* \propto Q_* \frac{\cos\beta}{\cos Z}. \tag{2}$$

A semi-empirical function was found to describe the above shown proportionality:

$$\Psi = f(Q_*, \beta, Z) = Q_* \left\{ \frac{\cos\beta}{\cos Z} + \left[\frac{\cos\beta}{\cos Z} \right]^2 \right\} \tag{3}$$

for positive Q_*. Because the differences between the horizontal and tilted measurements are insignificant when solar radiation is zero, Ψ is set equal to Q_* for negative net radiation.

Thereafter, the following regression between Ψ and Q_* was preformed for the site described in Matzinger et al. (2003),

$$Q'_* = a\Psi^2 + b\Psi + c, \tag{4}$$

where the parameters $a = 3.689 \times 10^{-5}$, $b = 0.5014$, and $c = 16.6187$ were found, which include local information. Because we have no data to calculate this regression ourselves and the sites are relatively similar, the measurements were made over grassland in an alpine valley as well, we used these parameters to calculate the slope parallel net radiation.

The reasoning behind such a correction is as follows. As the terrain around the weather station was almost flat, the horizontally installed net radiometer was approximately parallel to the underlying surface. Nevertheless, it cannot be completely ruled out that the direct incoming beam, which is part of the incoming shortwave radiation, might have been measured for the wrong slope inclination. Because we measured on a small terrace and the surrounding slopes are quite steep, the effective energy input might thus better correspond with that of the slope. Therefore, we corrected our data as described above in order to evaluate whether the energy input corresponds more with that for inclined surfaces. To calculate the solar declination, the algorithm by Whiteman and Allwine (1986) was used with an inclination angle of 25° and an azimuth of 205°.

2.6 Energy Budget Closure

The surface energy budget was defined as

$$Q_* - Q_G = Q_H + Q_E + \Delta Q, \tag{5}$$

where Q_* is net radiation measured with the CNR1 4-way radiometer or estimated by correcting for inclination angle as described above. Q_G is ground heat flux measured with the soil heat flux plates, and Q_H and Q_E are eddy-covariance fluxes for sensible and latent heat, respectively. The additional term ΔQ accounts for the budget closure gap and collects all

fluxes that are either not measured in the three-dimensional system of really complex topography (advective components and vegetation storage), or that are measured inaccurately. In a perfect one-dimensional steady-state world ΔQ is expected to be zero.

2.7 Footprint Model

For assessing the footprint area of our flux measurements we used the parameterized version of the Kljun et al. (2004) footprint model. For each 30-min period we computed the 80% footprint area and then collected all information in a regular $1 \times 1\,\mathrm{m}^2$ grid. For display, we used local polynomial regression fitting (loess function in R; see R Development Core Team 2006) on the two-dimensional data to yield smoothed contour lines. The contour levels were chosen to represent percentages of the maximum contribution in the matrix of footprint weights.

2.8 Light Response Curve

The light response curve describes the relation between the NEE and the photosynthetically active radiation measured as photosynthetic photon flux density (PPFD). Various empirical equations exist to describe this connection. We use the one introduced by Ruimy et al. (1995):

$$NEE(PPFD) = \frac{\alpha F_\infty PPFD}{\alpha F_\infty + PPFD} - R_{eco} \tag{6}$$

where $R_{eco}\,\mu\mathrm{mol\,m^{-2}\,s^{-1}}$ estimates the average respiration of the ecosystem. The term $F_\infty\,\mu\mathrm{mol\,m^{-2}\,s^{-1}}$ is the maximum possible assimilation rate at light saturation whereas the apparent quantum yield α describes how fast the photosynthesis responds to low light. The parameters R_{eco}, F_∞ and α were calculated by the nonlinear least-squares fitting function of the statistics program R (R Development Core Team 2006).

3 Results

3.1 Wind Field

Mountain climates are strongly determined by the inhomogeneous terrain. Valleys channel flows and surfaces heat differently according to the inclination of the slopes as well as shadows from surrounding mountains. Smaller topographic features may disturb air streams and produce additional turbulence. In general, it can be said that the climate of a certain place strongly depends on the local environment. As EC measurements have high requirements regarding the stationarity of the wind field, wind speed and wind direction are evaluated in more detail in this section.

Wind along the valley axis was predominant during 93% of the measurement period. Downvalley winds prevailed during 43% of the time whereas upvalley occurred during 50% of the measurements. Slope winds were very rarely observed, only 7% of the measurements showed evidence of slope winds, and if so, such conditions were always related to very low speeds (Fig. 3).

The prevailing wind directions present a pattern composed of three different modes shown in Fig. 4. Very dominant (58% of the measurement period) is the pattern where wind direction changes twice per day, once in the morning and once in the evening. During the short transition period, when winds change from upvalley to downvalley or vice versa (around

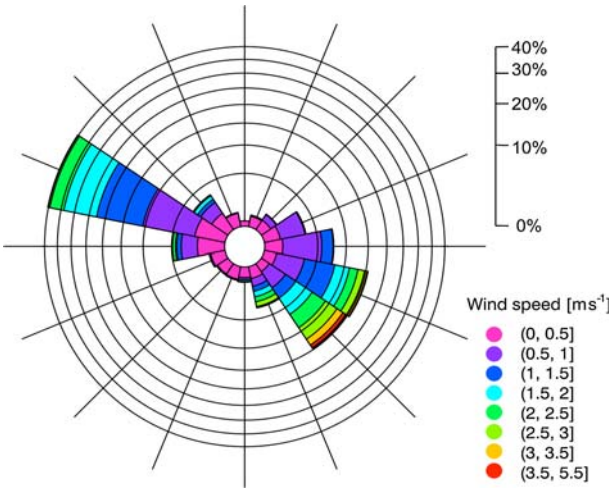

Fig. 3 Wind rose for the growing season 2006 on Crap Alv. The size of the sectors represents the frequency of the wind directions and the colours indicate the vectorial wind speed class

0900 and 2000–2100 h), slope winds sometimes become predominant. The wind speed is very low during this transition period. This pattern represents the textbook knowledge of the typical mesoscale phenomenon of the valley-wind system as described in Whiteman (2000).

The two other patterns shown in Fig. 4 are days when one wind direction was predominant during the whole day, either upvalley or downvalley. Normally, this pattern occurs for more than one consecutive day. Upvalley winds in such cases can be observed in combination with synoptic weather patterns of a west or north-west drift over central Europe that dominates the local wind system. This happened during 23% of the time during the measurement period. The observed persistent downvalley winds occur when Foehn conditions prevail within the Alps. While measuring, 15 out of 80 days with continuing east winds were observed.

For the assessment of EC measurements, not only the wind direction is of importance. The wind speed, turbulence, and stability of the atmosphere influence the flux footprint size. The diurnal pattern of the friction velocity u_* is as expected, with higher values during daytime when the atmospheric boundary layer is unstable (see Fig. 4). Even though positive values for the Monin-Obukhov stability parameter z/L are observed during the night, the magnitude is relatively small. This can be explained by the steady downvalley wind at night that reduces the probability of highly stable stratifications. Therefore, we obtain a relatively good representation of the pasture under investigation (Fig. 5) in the seasonal average. Most notably, the pass road is a purely touristic route that has almost no traffic at night that could potentially lead to erroneous nighttime flux measurements when downvalley winds prevail.

The presented contribution of prevailing winds described above is also reflected in the data quality: Fig. 6 shows clearly that more measurements were rejected during the transition periods under changing wind directions. Also during the night and periods with predominant winds from the west, the quality of the data is slightly lower.

3.2 Energy Budget Closure

According to the First Law of Thermodynamics, energy can be neither generated nor destroyed, and thus is conserved in a closed system. Therefore, the energy balance is

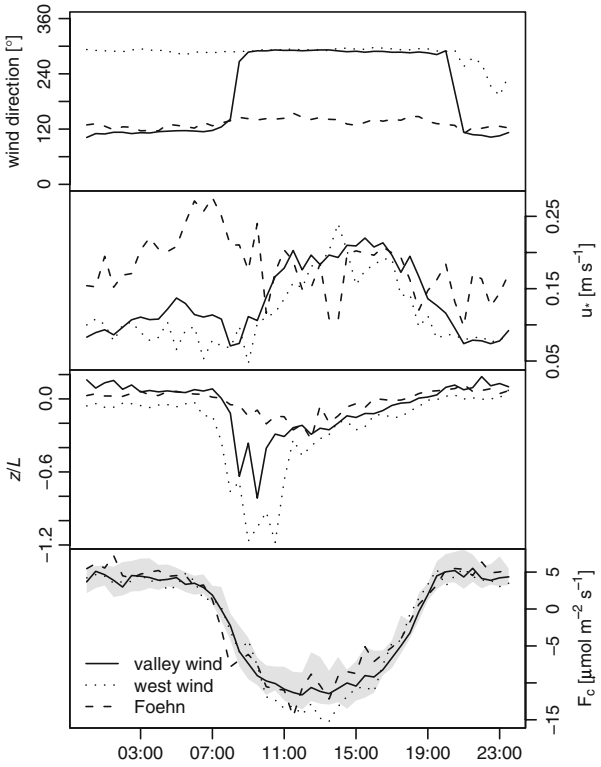

Fig. 4 Diurnal pattern of the wind direction, u_*, z/L and the CO_2 flux for the different weather pattern. The grey area in the bottom panel shows the inter quantile area for the flux during days with the valley wind system

considered a good measure to assess the performance of EC flux measurements. Figure 7 shows the correlation for the growing season 2006 on Crap Alv. The overall budget closure is $82 \pm 1\%$ (see Table 1). From the diurnal characteristics of energy imbalance in Fig. 8 we can see that the closure gap has a diurnal course with an energy surplus during part of the afternoon. Therefore, we also investigated the energy budget closure of morning and afternoon conditions separately (Fig. 7, Table 1).

We averaged all July data to yield the mean diurnal cycles presented in Fig. 8. Both variants with Q_* measured with horizontal sensors and Q_* corrected for slope aspect and angle are shown. This correction clearly reduces the amplitude of ΔQ as well as the timing of the maximum and minimum during the day. In the morning, the decrease in ΔQ is less prominent than in the afternoon. The crossing of the abscissa occurs later in the day and the absolute values in the afternoon are less negative.

3.3 CO_2 Fluxes

As the intention of this study is to assess whether the EC method might be an appropriate method to estimate NEE in topographic complex terrain, this section focuses on the CO_2 fluxes. A median daily cycle can be found in Fig. 4. Between the different wind regimes, no obvious difference can be found even though the wind field is different and the footprint area does not always cover the same patch of land.

EC measurements are known to underestimate the true flux during conditions with low turbulence that occur mostly during nighttime. Figure 9 compares the measured nighttime

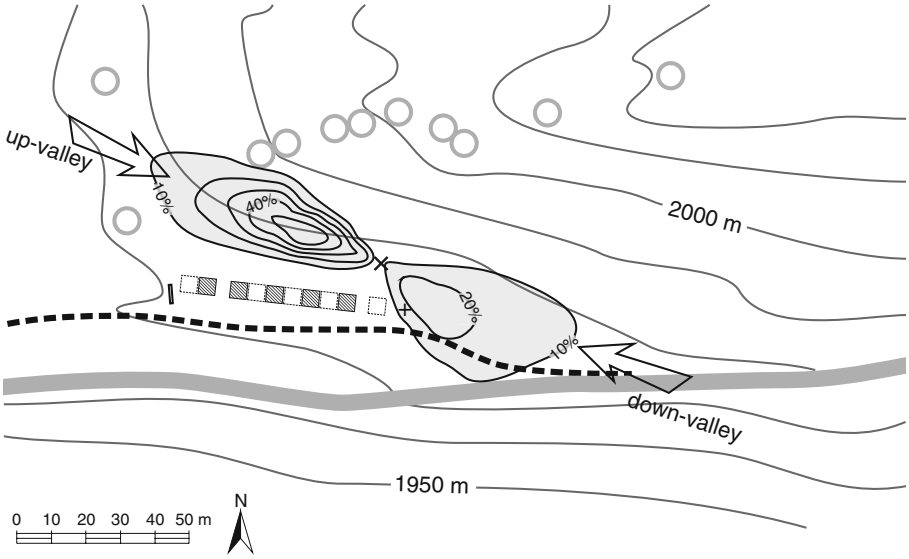

Fig. 5 Flux footprint area during the growing season 2006. Isolines show the percentage contribution with reference to the local point of maximum contribution, overlain over topographical contours at 10-m intervals. Hashed squares show locations of rain-exclusion shelters, and open squares show experimental control plots with different harvesting regime than the overall area. The rectangle represents a trough. Grey circles represent individual trees, thick grey line and black broken line represent paved road and unpaved access trail, respectively. The eddy flux tower is located between the two lobes of the footprint area. Roughly 70% of the grey shaded footprint area fall within the fenced area under investigation

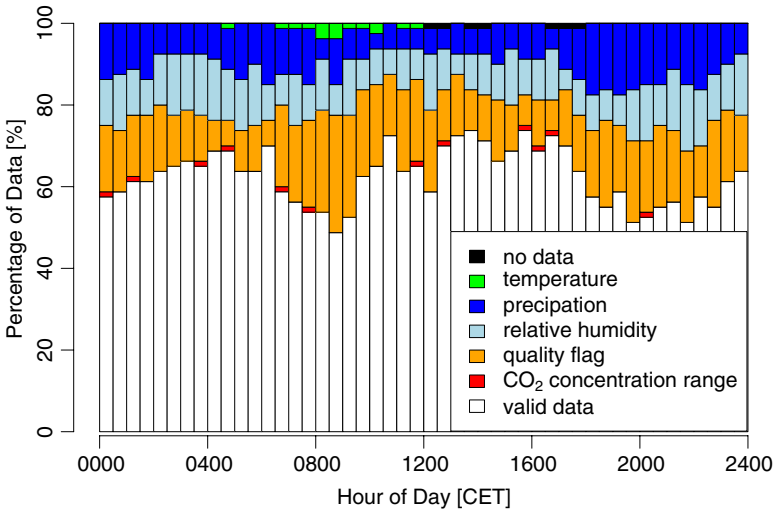

Fig. 6 Percentage of rejected and accepted records for every half-hour interval. The temperature filter rejected data when the difference between the temperature measured by the sonic anemometer and the air temperature from the weather station exceeded 5°C. Further, data were rejected during precipitation events and when the difference between air moisture obtained by the IRGA and the weather station exceeded 100 mmol m^{-3}. Then, all data were removed where the quality flag calculated by *eth-flux* was greather than one. Finally, all records where CO_2 concentration was outside the interval [11, 18] μmol m^{-3} were rejected

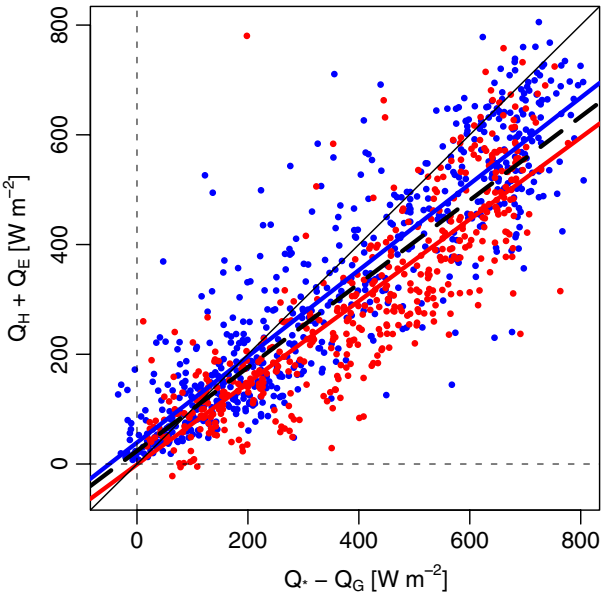

Fig. 7 Relation between available energy ($Q_* - Q_G$) and turbulent fluxes ($Q_H + Q_E$). Red points are morning observations (0800–1300 CET) whereas blue points were measured during the afternoon (1300–1800 CET). The colour lines represent the respective linear regression fit. The dashed line is the best fit to all measurements, and the black solid line shows the 1:1 ratio

Table 1 Linear best fits of turbulent fluxes ($Q_H + Q_E$) as a function of available energy ($Q_* - Q_G$) with net radiation Q_* measured perpendicular to the locally flat ground (top) and corrected for slope aspect and angle of the general topography

	Intercept (Wm^{-2})		Slope		R^2
	Best fit	Std. error	Best fit	Std. error	
All data	74.1	7.0	0.74	0.02	0.56
Morning values	−37.0	12.7	0.83	0.03	0.61
Afternoon values	85.8	6.2	0.94	0.02	0.77
All data, corrected Q_*	14.1	5.9	0.82	0.01	0.73
Morning values, corrected Q_*	−34.4	9.8	0.84	0.02	0.73
Afternoon values, corrected Q_*	37.0	6.8	0.84	0.02	0.79

All parameter estimates are highly significant ($p < 0.05$)

flux from the EC system with the estimated ecosystem respiration from light response curves. First, the data were binned into different temperature classes, each with a width of 2.5°C. For this step, the mean soil temperature for one day was used to make sure that daytime and nighttime data of each day belong to the same class. Thereafter, the mean value for nighttime fluxes (PPFD $<20\ \mu mol\,m^{-2}\,s^{-1}$) was calculated and the light response curve fitted for each class. The nighttime R_{eco} shows an increase with temperature and u_* but is usually smaller compared to the estimated respiration from the light response curve. An additional bar in Fig. 9 shows therefore the R_{eco} for values with an $u_* > 0.075\,m\,s^{-1}$ where the values are slightly higher than the unfiltered. In order to specify the u_* threshold, Fig. 10 shows a scatter plot of the soil respiration chamber measurements against the EC values. The graph shows a clear cut-off for low EC measurements. After removing all values with the u_* threshold as defined above (open symbols), most of these points disappear, too and a regression coefficient of 1.49 ± 0.06 ($p < 0.001$) could be found for the regression forced through the origin.

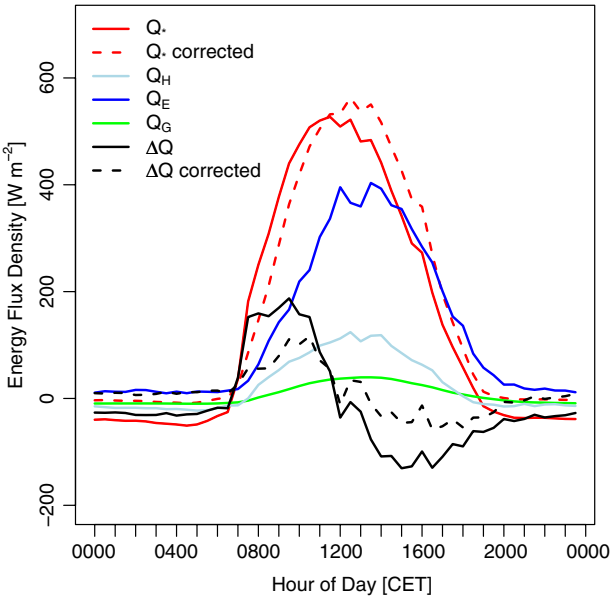

Fig. 8 Energy balance for July with the uncorrected and corrected net radiation and the resultant closure gap of the energy budget ΔQ

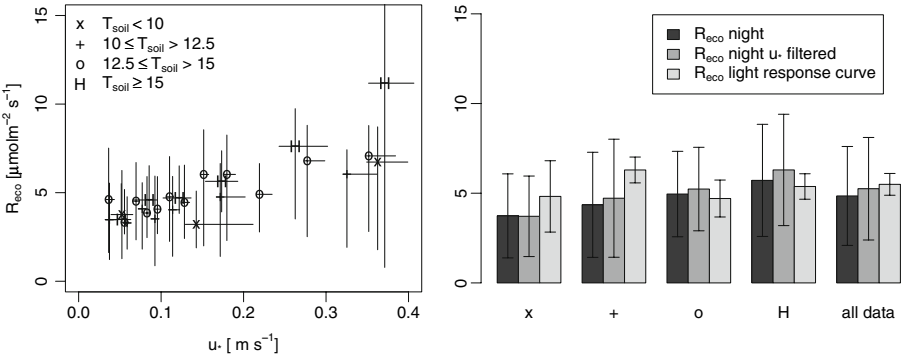

Fig. 9 Dependency of the ecosystem respiration on u_* and temperature. The left panel shows nighttime EC measurements (PPFD $< 20\mu\text{mol}\,\text{m}^{-2}\,\text{s}^{-1}$) against u_*. First, classes were built using the daily mean of the soil temperature. Thereafter, the data of each class were binned into subclasses of 30 values corresponding to their u_*. The right panel shows the mean nighttime respiration derived from EC measurements for each temperature class, once for all data and once for data with $u_* > 0.075\,\text{m}\,\text{s}^{-1}$. Further, the estimated R_{eco} from the light response curve for each class is shown as well. The error bars in both panels show one standard deviation

4 Discussion

4.1 Data Quality

Data quality was clearly affected by the valley-wind system, but not in an unacceptable way. During the transition period, when winds changed direction, more data were rejected by the quality flag (Fig. 6). Changes of wind direction by $\approx 180°$ cannot be considered stationary. Such conditions are represented by high variances of wind speed in the horizontal directions

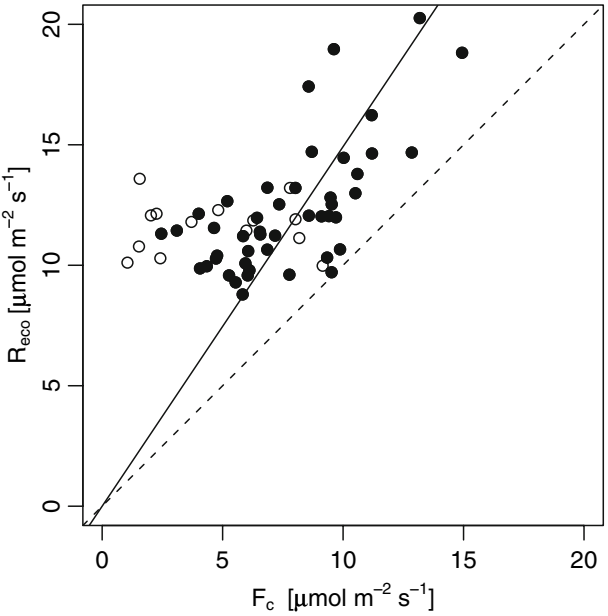

Fig. 10 Chamber versus nighttime EC measurements. The solid symbols represents the records with a $u_* > 0.075\,\mathrm{m\,s^{-1}}$ where the open points indicate points below this threshold. The solid line is the best fit to the solid points, and the dashed one shows the 1:1 ratio

and thus are identified as low-quality data periods. Note that in contrast to the assessment that Hammerle et al. (2007) made by plotting data rejection rates as a function of wind direction the variation is much lower at our site where we plotted the same information as a function of hour of day (our Fig. 6). This latter approach is statistically more robust because the possible number of samples is the same for each half-hour interval, whereas in the display used by Hammerle et al. (2007) the rare cases of unusual wind directions that are not along the main axis (in their case with a dominant slope-wind system it is the upslope and downslope direction, in our case it is the upvalley and downvalley direction) yield extremely poor statistics with high uncertainties.

During the night the data quality is lower, but only during the early night that is closely linked with the evening transition (1800–2400 h). The data rejection rates are similar to the rate observed during the morning transition period where up to 50% of all values had to be rejected. From Fig. 6 it appears that the data quality according to the CarboEurope standard, which is based on Foken and Wichura (1996), is as high during the late night (0200–0600 h) as during the early afternoon (1300–1700 h) where the upvalley wind system is fully developed and in near-steady-state conditions. Hammerle et al. (2007) found quite a different pattern at their slope-wind dominated locations in Austria. During daytime (wind directions around 90°) they accepted >80% of their values as high quality data (≈70% at our site), whereas during the night (wind directions around 300°) almost all measurements had to be rejected. In some sense this difference is not unexpected: our valley-wind dominated location has streamlines that are nearly horizontal along the height contours of the topography. Thus, for our location the assumptions made by the Monin–Obukhov similarity theory (MOST; Monin and Obukhov 1954) that forms the basis of the integral turbulence characteristics test used by Foken and Wichura (1996) can be expected to be similar to conditions over a flat surface. In contrast, the slope-wind system that dominates the sites

investigated by Hammerle et al. (2007) is additionally subject to local gravitational acceleration (downslope flows) and deceleration effects (upslope flows). They report poor correspondence between measured and theoretical σ_w/u_* during nighttime conditions and interpret this with a nearby roughness change from forest to grassland, without mentioning possible gravitational effects that are not included in the MOST. At our location there are a few scattered trees to both sides of the downvalley footprint (Fig. 5), which apparently do not reduce data quality as dramatically during the night as found by Hammerle et al. (2007) at their site that is bordered by closed forest. Although it would be premature to conclude a general rule from only two studies, we strongly suggest careful investigation of whether locations with predominant along-valley winds are less challenging for EC flux measurements than those with along-slope wind systems.

The precipitation flag in Fig. 6 also shows a diurnal course. In the long run, rainfall associated with synoptic weather systems should not exhibit such a diurnal course. This is related to local, convective rainfalls often accompanied by thunderstorms, which are known to be most frequent in the late afternoon and evening. This pattern is a typical phenomenon in the Alps and other high mountains.

4.2 Energy Budget Closure

Although closure of the energy budget is considered a quality check for EC measurements (Wilson et al. 2002), it is not included in the quality control procedure used in CarboEurope. When the closure gaps are small, the quality is assumed to be good whereas big gaps indicate underestimation or overestimation of components in the energy balance. The roughly 50 localities reviewed by Wilson et al. (2002) had energy budget closures in the range from 53 to 99% (mean 79%). Our values (Table 1) fit perfectly in the bulk part of these sites that are mostly located in far less complex topography. Thus, if we accept the energy budget criterion to be a quality measure of EC flux measurements in general, then we could argue that measurements carried out at our site with complex topography are of the same overall quality as those carried out over flat surfaces.

At our site, the energy budget closure shows a pronounced diurnal course that can generally be split into two parts. In the morning, the budget gap is positive while negative values occur especially during the afternoon but also during the night. This is the behaviour one expects over flat ground if instruments to measure net radiation were not levelled perfectly. In complex topography, it cannot easily be concluded whether this is the only or at least primary source of error. For example, Matzinger et al. (2003) compared horizontal and slope-parallel measured radiation fluxes for various slopes. Because of the changing angle between irradiance beam and the sensor, the values differ for the same site. Therefore, they concluded that radiances should be measured parallel to the slope to obtain correct values, as the energy entering into the natural environment should be measured.

In fact, our instrument was approximately mounted parallel to the slope as the terrace upon which we measured was almost flat. However, the surrounding slopes were steep and the energy input consequently different from that obtained on the terrace. The slope had an azimuth of 205° with an average inclination of about 25°. Correcting the flux for these parameters would imply a reduction of energy input in the morning and an increase in the afternoon. As this would explain part of our closure gap, we corrected the net radiation as described above. This correction is not perfect, but can be seen as a simple approach to explain the diurnal course of the energy budget closure (Fig. 8). Further, the determination of the slope length and therefore of the resulting inclination angle is very subjective (Whiteman et al. 1989). Nevertheless, the shape of the newly calculated net radiation is now closer to

the expected bell shape. Before, the net radiation curve was skewed with a steeper increase in the morning than the flatter decrease in the afternoon. The closure gap in the energy budget (ΔQ) is still evident, but now with a different diurnal course that agrees more with the conceptual knowledge that valley wind systems dislocate an air mass in one direction during the day and in the opposite direction at night. The course seen in Fig. 8 after correction can now be explained by the time lags between solar heating and these winds that always induce horizontal transport of air (advection).

The characteristics of advected air may differ from those of the site itself. The typical diurnal course of the differential heating in a nearby valley was described in full detail by Urfer-Henneberger (1970) and Urfer-Henneberger and Turner (1982). We thus can restrict our discussion to how these well-known mountain valley wind systems influence our local energy budget closure. In the morning, when cooler air is advected, energy is needed to heat it. This energy cannot be used to evaporate water and cannot be stored in the ground. The air also exits in the horizontal plain and hence fluxes are not measured by the EC method. The result is a measured energy input towards the surface that is larger than the output, thus a positive ΔQ is established. This is most prominent in the morning (Fig. 8 from sunrise until $\approx$1100 h) when east-exposed slopes heat faster than the flatter areas or the areas with a different exposure. This is the initialisation for the change of the main wind direction: first, slope winds develop, thereafter the whole valley wind system changes direction and cooler air from the lower part of the valley is transported upwards.

There are several possibilities why temperature varies greatly in a valley: (1) The advected air may have been part of the nighttime inversion and therefore is by definition cooler than the overlying air. (2) Steep mountains may shade the valley floor so the energy input is reduced to diffuse radiation for areas without direct irradiance at lower elevations in the valley. (3) The exposition and slope angle largely defines the amount of direct shortwave energy input received at the surface, which strongly determines how quickly it warms up relative to other locations in the valley. All these effects imply an upward transport of relatively cooler air along the valley axis and in the upslope direction.

As the day progresses, the upvalley wind becomes fully developed. In contrast to morning conditions, a certain amount of heat produced by the radiative energy received downwind of our EC flux site is now transported upvalley such that ΔQ becomes negative in the afternoon. This warm air advection acts as an extra energy source in addition to Q_* and Q_G.

Because of the pronounced diurnal course of ΔQ at our site we did not only look at the average linear regression of measured turbulent fluxes ($Q_H + Q_E$) versus available energy ($Q_* - Q_G$), but also looked at morning and afternoon conditions separately (Fig. 8). The regression line for the morning values is closest to the regression line for all values when energy input is high whereas the line for the afternoon values matches better when available energy is low. The slope of the regression using all data points increases from 0.74 to 0.82 after the correction, and the intercept decreases from 74.1 to 14.1 W m^{-2}, and the explained fraction of variance increases from 0.57 to 0.73. While the slope of our regression is well within the range observed by Wilson et al. (2002), our intercepts are only within the range of -32.9 to 36.9 W m^{-2} reported by Wilson et al. (2002) if we correct our net radiation measurements for slope inclination of the general topography. Turbulent energy fluxes normally lag the available energy in the diurnal course also at other locations (Wilson et al. 2002) and the energy budget is never closed in highly complex terrain (Rotach et al. 2003). As we have shown the energy budget closure criterion is not a firm measure of EC flux data quality. The questions of how to measure the radiative components is at least as important as the question about the validity of EC measurements.

Other reasons for the energy gap may exist, but cannot explain this magnitude and specially would not lead to the observed diurnal pattern. The storage terms of the soil and air have been corrected and the ogive shows (not presented) that after 1 min, already 99% of the flux is captured. The cospectra (see Fig. 2) show no obvious damping in the low frequency contribution and the damping-loss correction is applied for high frequency losses.

4.3 CO_2 Fluxes

As general data quality and energy budget closure do not show abnormal patterns compared with studies in less challenging terrain, this section focuses on the CO_2 fluxes.

The magnitude of the CO_2 fluxes is reasonable for this type of vegetation (Ruimy et al. 1995). However, most questionable are normally nighttime data when the atmospheric stratification is stable. Therefore, we compared the nighttime respiration (PPFD $<20\,\mu\mathrm{mol\,m^{-2}\,s^{-1}}$) to estimate ecosystem respiration derived from daytime data using the light response curve. Whereas R_{night} increases as expected with higher soil temperature, the R_{eco} from the light response curve does not show this pattern. Nevertheless, the R_{eco} values are considerably higher than the R_{night} . Therefore, we applied an additional u_* filter removing values with $u_* < 0.075\,\mathrm{m\,s^{-1}}$. The values after the filtering are now higher and sometimes exceed the estimated R_{eco} from the light response curve.

The comparison of EC with chamber measurements shows a similar result (see Fig. 10). The chamber values are relatively high, which might be related to problems determining the true chamber volume used in the computations. Nevertheless, we see a correlation between the two variables that tails off in the lower range. Most of these low values correspond to periods with low u_*. Because we can observe this tailing off, and it is explicable by lack of mixing due to low turbulence, we assume that our nighttime measurements have an appropriate quality if a low u_* threshold is exceeded. Therefore, an additional u_* filter should be applied for further analysis.

4.4 Choice of Location for Flux Measurements

The analysis of the prevailing wind presented herein showed that the wind system is mainly controlled by the mesoscale along-valley winds, whereas slope winds are almost irrelevant at this location. This has several implications for flux measurements. Due to the channelling effect of the topography, only the land cover along the valley direction influences the eddy-covariance flux measurements. The instrument fetch should be as homogeneous as possible in the upvalley and downvalley direction, whereas roughness and land cover changes in the lateral direction to this main axis are much less of concern for EC flux measurements. The main reason therefore is the change of the wind direction twice per day. Thus, the vegetation on both sides of the instruments should be similar if cumulative sums of CO_2 exchange shall represent a single land-use type. Further, the main wind directions should be considered when mounting the instruments. Slope winds hardly exceeded $0.5\,\mathrm{m\,s^{-1}}$ in our case and thus did not require special filtering. With such weak winds, the footprint area is so small and close to the EC tower that fetch limitations do not appear to be of concern for seasonal NEE sums.

5 Conclusions

The eddy-covariance method has high requirements regarding the environmental conditions. Even for study sites with ideal conditions, it is difficult to fulfil all of them. Therefore, it does

not surprise that some requirements are not completely satisfied in highly complex terrain. In valley systems, the local wind system has a considerable impact on the measurements. The continuous wind along the valley axis, upvalley during the day and downvalley by night, certainly involves horizontal advection. This is however not specific to our locality in complex topography, and energy budget closure was found to lie in the range reported from many other locations that are considered more ideal for EC flux measurements.

We could not find any indication that the EC method does not work in complex terrain. The daily averaged energy imbalance of $9.5\,\mathrm{W\,m^{-2}}$ (or $0.82\,\mathrm{MJ\,day^{-1}}$) is only $\approx$8% of the average net radiation and indicates that high quality flux measurements are also possible at such locations with challenging topography. An important prerequisite is, however, the careful examination of local conditions, especially channelling effects of the prevailing winds by local topography. Our suggestion is to look for locations that have the prevailing winds along the local contour lines, if possible. Due to the typical along-valley (or along-slope) wind system in complex terrain, which changes direction twice daily in a non-random way, it is essential that the footprint area in both prevailing wind directions are representative for the same ecosystem under investigation.

Assuming that our findings for the energy budget closure can also be translated to CO_2 flux measurements we argue that NEE measurements that were carried out simultaneously are expected to be of similarly high quality. To fully confirm these findings, a more sophisticated study with several towers in order to measure three-dimensional fluxes would be needed.

Acknowledgements This project was supported by the Swiss National Science Foundation, grant 200021-105949. We thank the two technicians Jürg Schenk (University of Bern) and Peter Plüss (ETH Zurich) for their support in preparation and installation of all equipment. Special thanks go to Natascha Kljun (ETH Zurich) for making the Fortran source code of her footprint model available to us, to Rolf Philipona (MeteoSwiss) who supported us with radiation instrument calibration, and to Joseph P. McFadden (University of Minnesota, St. Paul) who strongly helped us to improve this paper. We also thank three anonymous reviewers for their valuable comments and critical feedbacks.

References

Baldocchi D (2003) Assessing the eddy-covariance technique for evaluating carbon dioxide exchange rates of ecosystems: past, present and future. Global Change Biol 9(4):479–492

Barr AG, King KM, Gillespie TJ, den Hartog G, Neumann HH (1994) A comparison of Bowen ratio and eddy correlation sensible and latent heat flux measurements above deciduous forest. Boundary-Layer Meteorol 71:21–41

Bearth P, Heierli H, Roesli F, Gesellschaft SN (1987) Geologischer Atlas der Schweiz, 1237 Albulapass, Atlasblatt 82. Bundesamt für Landestopographie, Bern

Caflisch C (1954) Weissenstein am Albula: Crap Alv 1654–1954. Bündner Monatsblatt, Zeitschrift für bündnerische Geschichte, Landes- und Volkskunde 105(2):65–111

Eugster W, Senn W (1995) A cospectral correction model for measurement of turbulent NO_2 flux. Boundary-Layer Meteorol 74(4):321–340

Eugster W, Kling G, Jonas T, McFadden JP, Wüest A, MacIntyre S, Chapin FS III (2003) CO_2 exchange between air and water in an arctic Alaskan and midlatitude Swiss lake: Importance of convective mixing. J Geophys Res 108(D12):4362–4380. doi:10.1029/2002JD002653

Foken T, Wichura B (1996) Tools for quality assessment of surface-based flux measurements. Agric Forest Meteorol 78(1):83–105

Hammerle A, Haslwanter A, Schmitt M, Bahn M, Tappeiner U, Cernusca A, Wohlfahrt G (2007) Eddy covariance measurements of carbon dioxide, latent and sensible energy fluxes above a meadow on a mountain slope. Boundary-Layer Meteorol 122(2):397–416

Kaimal J, Wyngaard J, Izumi Y, Cote O (1972) Spectral characteristics of surface-layer turbulence. Quart J Roy Meteorol Soc 98(417):563–589

Keller P (2006) Vegetationskundliche Untersuchungen und Ertrag der Grünlandflächen im Gebiet der ETH-Forschungsstation Alp Weissenstein GR. Master's thesis, Geographical Institute, University of Zurich, 63 pp.
Kljun N, Calanca P, Rotach MW, Schmid HP (2004) A simple parameterisation for flux footprint predictions. Boundary-Layer Meteorol 112:503–523
Matzinger N, Andretta M, van Gorsel E, Vogt R, Ohmura A, Rotach M (2003) Surface radiation budget in an alpine valley. Quart J Roy Meteorol Soc 129(588):877–895
Mauder M, Foken T, Clement R, Elbers JA, Eugster W, Grünwald T, Heusinkveld B, Kolle O (2007) Quality control of CarboEurope flux data — Part II: Inter-comparison of eddy-covariance software. Biogeosciences Discuss 4:4067–4099
McMillen R (1988) An eddy correlation technique with extended applicability to non-simple terrain. Boundary-Layer Meteorol 43(3):231–245
Monin AS, Obukhov AM (1954) Osnovnye zakonomernosti turbulentnogo peremešivaniâ v prizemnom sloe atmosfery. Trudy geofiz inst Akad Nauk SSSR 24(151):163–187 (in Russian)
Oke T (1987) Boundary layer climates. Methuen, London, 435 pp
R Development Core Team (2006) R: A language and environment for statistical computing. R foundation for statistical computing, Vienna, Austria, URL http://www.R-project.org, ISBN 3-900051-07-0
Rogiers N (2005) Impact of site history and land-management on CO_2 fluxes at a grassland in the Swiss pre-alps. PhD thesis, University of Bern, 177 pp.
Rotach M, Calanca P, Weigel A, Andretta M (2003) On the closure of the surface energy balance in highly complex terrain. ICAM/MAP 37:247–250
Ruimy A, Jarvis P, Baldocchi D, Saugier B (1995) CO_2 fluxes over plant canopies and solar radiation: a review. Adv Ecol Res 26: 1–68
Stull RB (1988) An introduction to boundary layer meteorology. Kluwer Academic Publishers, Dordrecht, 666 pp.
Urfer-Henneberger C (1970) Neuere Beobachtungen über die Entwicklung des Schönwetterwindsystems in einem V-förmigen Alpental (Dischmatal bei Davos). Arch Meteorol Geophys Bioklimatol 18:21–42
Urfer-Henneberger C, Turner H (1982) Bodennahes Windsystem und Temperaturgradienten bei verschiedenen Wetterlagen in einem von Süden nach Norden führenden V-förmigen Alpental. Arch Meteorol Geophys Bioklimatol B 31:253–271
van der Molen MK, Zeeman MJ, Lebis J, Dolman AJ (2006) Eclog: a handheld eddy-covariance logging system. Comput Electron Agric 51(1–2):110–114
Webb EK, Pearman GI, Leuning R (1980) Correction of flux measurements for density effects due to heat and water vapour transfer. Quart J Roy Meteorol Soc 106(447):85–100
Whiteman C, Allwine K (1986) Extraterrestrial solar radiation on inclined surfaces. Environ Softw 1(3): 164–174
Whiteman C, Allwine K, Fritschen L, Orgill M, Simpson J (1989) Deep valley radiation and surface energy budget microclimates. Part I: Radiation. J Appl Meteorol 28(6):414–426
Whiteman CD (2000) Mountain meteorology fundamentals and applications. Oxford University Press, 355 pp.
Wilson K, Goldstein A, Falge E, Aubinet M, Baldocchi D, Berbigier P, Bernhofer C, Ceulemans R, Dolman H, Field C, Grelle A, Ibrom A, Law BE, Kowalski A, Meyers T, Moncrieff J, Monson R, Oechel W, Tenhunen J, Valentini R, Verma S (2002) Energy balance closure at fluxnet sites. Agric Forest Meteorol 113(1–4):223–243